JARO 16: 317–329 (2015)
DOI: 10.1007/s10162-015-0513-0

JARO
Journal of the Association for Research in Otolaryngology

Research Article

Tuning of SFOAEs Evoked by Low-Frequency Tones Is Not Compatible with Localized Emission Generation

Karolina K. Charaziak[1,2] and Jonathan H. Siegel[1]

[1]*Roxelyn and Richard Pepper Department of Communication Sciences and Disorders, Northwestern University, Evanston, IL, USA*
[2]*Eaton-Peabody Laboratories, Massachusetts Eye and Ear Infirmary, Boston, MA, USA*

Received: 5 June 2014; Accepted: 17 February 2015; Online publication: 27 March 2015

ABSTRACT

Stimulus-frequency otoacoustic emissions (SFOAEs) appear to be well suited for assessing frequency selectivity because, at least on theoretical grounds, they originate over a restricted region of the cochlea near the characteristic place of the evoking tone. In support of this view, we previously found good agreement between SFOAE suppression tuning curves (SF-STCs) and a control measure of frequency selectivity (compound action potential suppression tuning curves (CAP-STC)) for frequencies above 3 kHz in chinchillas. For lower frequencies, however, SF-STCs and were over five times broader than the CAP-STCs and demonstrated more high-pass rather than narrow band-pass filter characteristics. Here, we test the hypothesis that the broad tuning of low-frequency SF-STCs is because emissions originate over a broad region of the cochlea extending basal to the characteristic place of the evoking tone. We removed contributions of the hypothesized basally located SFOAE sources by either pre-suppressing them with a high-frequency interference tone (IT; 4.2, 6.2, or 9.2 kHz at 75 dB sound pressure level (SPL)) or by inducing acoustic trauma at high frequencies (exposures to 8, 5, and lastly 3-kHz tones at 110–115 dB SPL). The 1-kHz SF-STCs and CAP-STCs were measured for baseline, IT present and following the acoustic trauma conditions in anesthetized chinchillas. The IT and acoustic trauma affected SF-STCs in an almost indistinguishable way. The SF-STCs changed progressively from a broad high-pass to narrow band-pass shape as the frequency of the IT was lowered and for subsequent exposures to lower-frequency tones. Both results were in agreement with the "basal sources" hypothesis. In contrast, CAP-STCs were not changed by either manipulation, indicating that neither the IT nor acoustic trauma affected the 1-kHz characteristic place. Thus, unlike CAPs, SFOAEs cannot be considered as a place-specific measure of cochlear function at low frequencies, at least in chinchillas.

Keywords: acoustic trauma, two-tone suppression, compound action potential, suppression tuning curve, chinchilla

INTRODUCTION

Since their discovery over three decades ago, otoacoustic emissions (OAEs) have served as a window to cochlear processing, despite rather limited understanding on how OAEs are generated, shaped, and propagated out of the cochlea (reviewed in Kemp 2007). One route to get more insight into OAE generation processes is to relate them to known features of the active cochlea, such as frequency selectivity.

Cochlear frequency selectivity is usually characterized with frequency-threshold tuning curves from the basilar membrane or single auditory nerve fibers, but it can be also approximated well with the less invasive measures of compound action potential suppression tuning curves (CAP-STCs; reviewed in Ruggero and Temchin 2005; Charaziak and Siegel 2014). This is not surprising, as the CAP evoked by a low-level tone burst represents responses from auditory nerve fibers

Correspondence to: Karolina K. Charaziak · Eaton-Peabody Laboratories · Massachusetts Eye and Ear Infirmary · Boston, MA, USA. email: KarolinaCharaziak2013@u.northwestern.edu

innervating a small region near the characteristic frequency (CF) place of the stimulus (Teas et al. 1962; Özdamar and Dallos 1978). Similarly, STCs can be measured for stimulus-frequency (SF) OAEs evoked by fixed low-level pure tones. It was expected that SF-STCs would closely resemble the shapes of CAP-STCs (Charaziak and Siegel 2014), as SFOAEs evoked by low-level probe tones have also been hypothesized to originate near the CF place of the evoking tone (Zweig and Shera 1995). While this relationship seemed to hold at high probe frequencies (>3 kHz) in chinchillas, at lower frequencies SF-STCs were over five times broader than CAP-STCs. Thus, at low frequencies, SF-STCs did not reflect tuning of the cochlear filters even for low-level probe tones. Such broad, essentially high-pass tuning at low frequencies has been previously reported for cochlear microphonics (CM) STCs in mice, and it was explained by the dominance of round-window CM by hair cell receptor currents produced basal to the stimulus CF place (Cheatham et al. 2011a). Given some similarities between SFOAE and CM suppression (Siegel 2006), it is hypothesized that the broad high-pass tuning of low-frequency SF-STCs was due to SFOAE originating not only near the CF place of the probe but also basal to it (i.e., "basal" SFOAE sources; Guinan 1990; Siegel et al. 2005; Choi et al. 2008). The extended region of OAE generation may also explain high-pass tuning, irregular shapes, and secondary lobes of suppression/enhancement reported for STCs measured in certain conditions for other types of evoked emissions and/or in different species (Kemp and Chum 1980; Martin et al. 1999; Mills 2000; Martin et al. 2003; Zettner and Folsom 2003; Charaziak et al. 2013). Removing contributions from basal OAE sources should result in narrow OAE-STC tuning as observed for responses generated in the CF region, such as CAPs. In this study, we test this prediction in chinchillas using two approaches designed to reduce SFOAE generation basal to the CF place of the low-frequency probe (1 kHz) without affecting the CF place itself. These consisted of suppressing the hypothesized basal SFOAE sources with a high-frequency interference tone (IT) or creating sound-induced high-frequency threshold shifts (acoustic trauma).

Suppression paradigms have been used previously to gauge the generation site of cochlear responses to stimuli for different types of OAEs as well as CM and CAPs (e.g., Teas et al. 1962; Heitmann et al. 1998; Martin et al. 1999; Cheatham et al. 2011a; He et al. 2012). A suppressor can drive the mechanotransducer currents of OHCs into saturation, resulting in a reduced response to the probe stimulus (e.g., Geisler et al. 1990). When applied to OAEs, the suppressor is assumed to remove/diminish contributions from OAE sources located in the region of large excitation produced by the suppressor, especially near its CF place (e.g., Guinan 1990; Brass and Kemp 1993; Martin et al. 1999; 2003). Thus, if the broad tuning of SF-STCs reflects contributions from basally located SFOAE sources, introducing a fixed high-frequency tone, referred to here as an IT to differentiate from suppressor tones of varying frequencies used to measure a STC, should suppress the basal sources and consequently change the shape of SF-STC to narrow band-pass tuning.

It is well established that excessive exposure to sounds deteriorates cochlear structure and processes, those of OHCs in particular (e.g., Thorne et al. 1986; Liberman and Dodds 1987; Pickles et al. 1987; Puel et al. 1988; Davis et al. 1989; Nordmann et al. 2000). If the OAE generation process is linked to OHC function at a given cochlear location, introducing localized damage/interruption of OHC function via acoustic overstimulation should reveal the spatial extent of OAE sources. This method has been used for investigating contributions from spatially distributed OAE sources in the case of transient-evoked (TE) OAEs (Avan et al. 1995; Withnell et al. 2000) as well as distortion-product (DP) OAEs (Martin et al. 2010).

In this study, the effects of the ITs and acoustic trauma were measured for 1-kHz SF-STCs, which consistently demonstrated broad tuning in chinchillas (Charaziak and Siegel 2014). We used three IT conditions (at 9.2, 6.2, or 4.2 kHz and 75 dB sound pressure level; SPL) and three tonal overexposure conditions (8, 5, and 3 kHz at 110–115 dB SPL, in sequence) in the same animal. If the effects of ITs and acoustic trauma are similar, then the former approach could be used to minimize contributions from basal SFOAE sources rapidly and noninvasively. Due to the sharp apical cutoff of the basilar membrane traveling wave, neither of these manipulations was expected to affect the 1-kHz CF place, as assessed via measurements of 1-kHz CAP-STCs. If the broad tuning of SF-STCs was due to contributions from basally located OAE sources, we expected that either manipulation would narrow the tuning of SF-STCs.

METHODS

Animal Preparation

The experiments were carried out in deeply anesthetized male adult chinchillas (21, with a subset of seven animals included in the acoustic trauma part of the experiment). The anesthesia was induced with ketamine hydrochloride (20 mg/kg, injected subcutaneously) followed by an initial dose of Dial (diallylbarbituric acid or allobarbital, 50 mg/kg) in urethane (200 mg/kg) that eliminated limb withdrawal reflexes. Supplementary doses of Dial in urethane (20 % of the

initial dose) were administered as needed to maintain the depth of anesthesia. The animal preparation procedures were as detailed in Charaziak and Siegel (2014). Briefly, the animals were tracheotomized, the head was immobilized in a head holder, and the cartilaginous part of the ear canal and pinna and the lateral portion of the bony meatus were removed to visualize the tympanic membrane. The tip of the OAE probe was placed near the tympanic membrane and sealed to the bony rim of the ear canal with an impression material. A silver ball electrode (for CAP recordings) was placed near the round window via a posterior opening in the bulla. The reference electrode was placed in the skin of the contralateral ear, and the ground electrode was attached to the head holder. In all animals, the tendon of the tensor tympani was sectioned and, in ten animals, the stapedius muscle was additionally paralyzed by sectioning the facial nerve between its genu and the stapedial nerve branch (Songer and Rosowski 2005). Note, in previous research (unpublished), we did not find large changes in CAP thresholds or OAE levels before and after paralyzing the stapedius muscle. In this study, disabling the stapedius muscle did not appear to influence susceptibility of the animal to inducing high- to mid-frequency threshold shifts via acoustic overexposure (Table 1; compare exposure durations for animals with/without superscript mark). All animal procedures were approved by the Animal Care and Use Committee of Northwestern University.

Instrumentation

The sound was delivered via two modified Radio Shack RS-1377 Super Tweeters coupled via Tygon plastic tubing to an Etymōtic ER-10S OAE probe (a customized version of the four-microphone ER-10A). The high-intensity tones used to induce sensitivity loss were presented via a Fostex FT17H Horn Super Tweeter driven by a Symetrix 420 power amplifier and coupled to the ear canal through one of the sound delivery tubes with the emission probe in place. The output from the OAE microphone pre-amplifier and from the CAP pre-amplifier (custom built) was high-pass-filtered (with a corner frequency of 155 and 100 Hz, respectively) and fed differentially to separate channels of a 24-bit sound card (Card Deluxe-Digital Audio Labs). The acoustical signals were generated digitally with a sample rate of 44.1 kHz (buffer size 4096) in EMAV software ver. 3.24 (Neely and Liu 2011) and with a sample rate of 88.2 kHz (buffer size 4096) in the custom software (written in Visual Basic 6.0, Microsoft Corp.). The stimulus levels were controlled in situ based on the ear canal responses to a constant amplitude chirp stimulus (~85 dB SPL) obtained separately for each channel with an OAE probe microphone. The sound pressure levels of stimuli and OAEs were compensated for the microphone transfer function of the OAE probe (Siegel 2007). The recordings were obtained in an electrically shielded sound-attenuating booth.

TABLE 1

The duration and intensity of tonal exposures at 8, 5, and 3 kHz resulting in at least 70 dB SPL CAP thresholds at ~9, 6, and 4 kHz, respectively

	Total exposure duration (min)/tone level (dB SPL)		
	Tone frequency		
ID	8 kHz	5 kHz	3 kHz
JN193[a]	18/110	12/110	12/110
JL083[a]	9/110	12/110	24/110
JL153[a]	9/110	12/110	24/110
JL183[a]	21/110 and 12/115	12/110	12/110
AG013	18[b]/110	24/110	24/110
AG223	9/110	12/110	12/110
OT013	18/110	12/110	12/110

[a]Stapedius muscle paralyzed

[b]For half of the time, tone frequency was changed to 9 kHz to induce larger CAP threshold shift at the highest frequencies that were little affected by the exposure to 8 kHz

Procedures

The experiment usually lasted about 13 h including animal preparation (~2 h) and data collection (baseline measures and the two manipulations). The first manipulation focused on collecting STCs in the presence of ITs of different frequencies (~4 h), while the second manipulation consisted of a series of three exposures to high-intensity tones (~7 h). Because the effects of the acoustic overexposures lasted longer than the duration of the experiment, the IT-STCs were obtained first. The state of the preparation was monitored throughout the experiment via recordings of CAP thresholds, SFOAEs level versus frequency functions (both described below) and low-level DPOAEs measured at $2f_1-f_2$, with $L_1/L_2=35/50$ dB SPL, $f_2/f_1=1.2$ and with f_2 varied from 0.5 to 20 kHz with resolution of 10 points per octave (p/oct; data not reported).

CAP Recordings. CAP amplitude was measured as the peak-to-peak amplitude of N1 (averaged over 64 presentations of 10-ms tone burst stimuli including 1-ms rise-fall time, alternating polarity, repetition frequency of 21 Hz). The CAP thresholds were measured automatically with a tracking procedure as the lowest SPL that evoked a criterion response of 10 μV for probe frequencies from 0.5 or 1 to 20 kHz (3 p/oct) for monitoring purposes and from 0.8 or 1 to 20 kHz (6 p/oct) when assessing the effect of the tonal

exposures on CAP thresholds. The tracking procedure adjusted the tone burst level until the CAP response was equal to the criterion (±1 dB). The amplitude of the tone burst was then decreased/increased in 2 dB steps so that a four-point input-output (IO) function around the criterion threshold was obtained. Solving the linear regression fit to the IO function for the criterion of 10 μV was taken as the CAP threshold. If the CAP threshold could not be measured at a given frequency, it was arbitrarily assigned to 95 dB SPL (the maximal allowed stimulus level).

The CAP-STCs were collected as iso-response curves for a fixed tone burst probe (f_{probe}) as a function of the frequency of a tonal suppressor, f_{sup} (custom software) using a simultaneous masking paradigm to best mimic the paradigm used to measure SF-STCs described below. For each f_{sup}, the suppressor level was varied automatically until the peak-to-peak magnitude of N1 was reduced by 3 dB (±1 dB; a decrement criterion). The center frequency of the tone burst was always equal to the f_{probe} used for SF-STC recordings (see below). The probe level was adjusted to produce a CAP magnitude exceeding threshold (typically ~20 μV) based on CAP IO functions (in 1 dB steps) measured briefly before CAP-STC measurements. The f_{sup} was varied from $0.5f_{probe}$ to $2f_{probe}$ with a resolution of 7 p/oct. Data collection was automatically terminated when the suppressor level reached 95 dB SPL, and no response meeting the threshold criterion was found.

SFOAE Measurements. The SFOAEs were extracted from the stimulus pressure using the suppression method (e.g., Brass and Kemp 1993; Kalluri and Shera 2007). The SFOAE residual at the probe frequency was calculated as the vector difference between the averaged responses (two repetitions each) to the probe tone (f_{probe}) and to the probe tone in the presence of the suppressor (f_{sup}). For measurements of SF-STC with an IT present, the residual was calculated as the difference between responses to f_{probe}+IT and f_{probe}+IT+f_{sup}. Thus, the SFOAE residual corresponds to the part of the SFOAE suppressed by f_{sup}. Trials demonstrating noise that exceeded a rejection criterion were automatically repeated. The phase of the f_{probe} stimulus was measured and subsequently subtracted from the phases of the SFOAE residuals to compensate for the stimulus delay. The SFOAE were expressed as the equivalent magnitude and phase of a tone that would have produced the measured change in the probe response (Guinan 1990).

When measured across a wide range of frequencies, the SFOAE level demonstrates an individualized pattern of peaks and valleys referred to as fine structure. To assure optimal signal to noise ratio for SF-STC measurements, the probe frequency was individually adjusted as the frequency that evoked the largest SFOAE near the nominal frequency of 1 kHz. The SFOAE fine structure was characterized with SFOAE measurements obtained using EMAV (f_{probe} varied from 0.5 to 16 kHz in 86 Hz steps fixed at 30 dB SPL, $f_{sup}=f_{probe}-43$ Hz, fixed at 65 dB SPL). This measurement was also used to monitor SFOAE levels throughout the experiment.

The SF-STCs were measured as iso-residual curves as a function of f_{sup} for a fixed f_{probe} (Charaziak et al. 2013; Charaziak and Siegel 2014). For a fixed probe and f_{sup}, the suppressor level was varied automatically until the SFOAE residual was within ±1 dB of the residual criterion (0 dB SPL). The f_{sup} was varied from $0.9f_{probe}$ to $6f_{probe}$ with a resolution of 10 p/oct and with decreased resolution to 5 p/oct in the range from $0.4f_{probe}$ to $0.9f_{probe}$. The f_{sup} was never allowed to be a harmonic or a subharmonic of f_{probe}. SFOAE residual criterion of 0 dB SPL was found to be small enough to detect small SFOAEs from distributed sources but large enough to guarantee a good signal to noise ratio. To approximately equalize the STC criteria for CAPs and SFOAEs (decrement vs residual criterion), we collected SF-STCs at a probe level producing an SFOAE level of about 10.7 dB SPL (established based on the SFOAE IO function, in 1 dB steps, with $f_{sup}=f_{probe}-43$ Hz, fixed at 65 dB SPL). The suppressor level that produced a 3-dB drop in the probe response (the amplitude changed by $\frac{1}{\sqrt{2}}$) produced a 10.7-dB drop in the residual response because $20\log_{10}\left(1-\frac{1}{\sqrt{2}}\right) = -10.7$ dB. Thus, a 3 dB decrement criterion for the probe-alone response (used for CAP-STCs) corresponded to −10.7-dB drop *re* the saturated residual response (i.e., estimate of total SFOAE).

High-Frequency Interference Tones. The SF-STCs and CAP-STCs were measured in the presence of additional high-frequency ITs set at nominal frequencies of either 9.2, 6.2, or 4.2 kHz at 75 dB SPL. The nominal frequencies of the ITs were picked (based on pilot data) to correspond to the frequencies affected most by exposures to high-intensity tones (at 8, 5, and 3 kHz, respectively). The IT frequency was individually adjusted to never be a harmonic of the f_{probe} and that intermodulation products created by interactions between f_{sup} and ITs were not at the frequency of f_{probe}, so that $n\cdot(f_2-f_1)\neq f_{probe}$, where n is an integer from 1 to 8, and $f_2>f_1$. For the 4.2- and 6.2-kHz ITs, the adjustments were less than ±0.04 % around the nominal frequency, while for the 9.2 kHz, larger adjustments were sometimes necessary (on average by 0.6 %, ranging from −2.2 to 9.8 %). The STCs obtained in the presence of an IT were measured with the same procedures as the baseline STCs (the IT off, see above) in a random order.

Tonal Overexposures. The acoustic trauma was induced by exposure to high-intensity tones (110–115 dB SPL) over a time period that resulted in an elevation of the CAP threshold to at least 70 dB SPL at and above the targeted frequencies (~9, 6, and 4 kHz following 8, 5, and 3 kHz of exposures, respectively). The intense tones were presented in 9 or 12 min time blocks until the desired CAP threshold shift was achieved (see Table 1 for exposure parameters for each animal). The tonal overexposures were applied in sequence from the highest to the lowest exposure frequency as it was easier to control the low-frequency extent of the CAP threshold shift than shifts at frequencies higher than the exposure tone (Ruggero et al. 1996). The STCs were measured following each exposure for the same f_{probe} as the baseline STCs (although in some cases the probe level had to be re-adjusted to meet the criteria described above; listed in Table 2).

Data Analyses. To quantitatively assess the effects of experimental manipulations on the shapes of STCs, low-side and high-side corner frequencies (f_{cor}) were calculated. For CAP-STCs, the low-/high-side f_{cor} was calculated as the lowest/highest suppressor frequency (in oct *re* f_{probe}) at which the suppressor level at the criterion threshold was 10 dB above the CAP-STC minimum (i.e., high-side f_{cor}−low-side f_{cor}=STC bandwidth across its widest range). For SF-STCs, f_{cor} was calculated in the same way with the exception that the STC minimum was defined as the lowest point of the curve for f_{sup}<1 oct *re* f_{probe}. This limitation was applied to avoid ambiguities in defining a tip for curves with broad high-pass shapes (e.g., see Fig. 1A).

The significance of changes in corner frequencies of STCs due to experimental manipulations was tested with a two-way (2×2) univariate analysis of covariance adjusted for the correlations between repeated measures within an animal (mixed-design ANCOVA).

TABLE 2

The probe levels used for SF-STC and CAP-STC measurements prior (baseline) and following the exposures to intense tones

	Probe level (dB SPL) Baseline/post-8 kHz/post-5 kHz/post-3 kHz	
ID	SF-STC	CAP-STC
JN193	39/43/39/42	45/45/45/50
JL083	43/35/36/35	59/60/61/65
JL153	45/45/45/42	68/68/68/70
JL183	29/48/48/47	50/67/67/65
AG013	30/47/48/59	40/50/52/55
AG223	35/42/48/50	52/54/56/57
OT013	30/32/51/46	35/50/55/51
Average	**36/42/45/46**	**50/56/58/59**

The level of the probe was individually adjusted to produce a predefined criterion response (see Methods section)

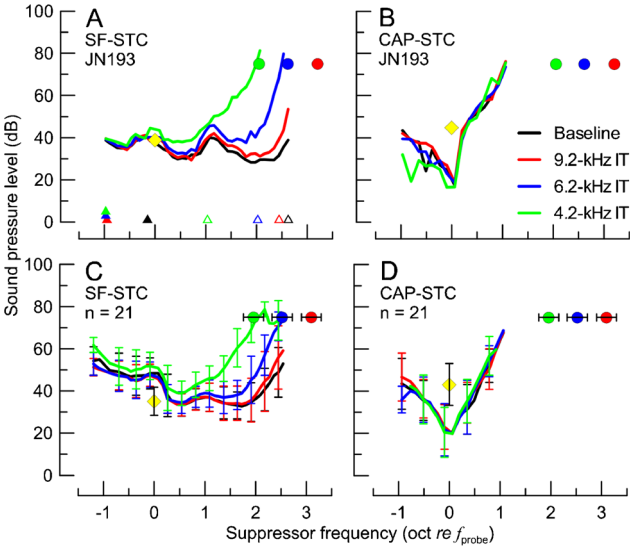

FIG. 1. The SF-STCs and CAP-STCs obtained in the absence (*black*) or presence of IT at varying frequencies (*red*: 9.2 kHz, *blue*: 6.2 kHz, *green*: 4.2 kHz) in one animal (**A**, **B**) and averaged across 21 animals (**C**, **D**). The frequencies and levels of the probe and the IT conditions are shown with *yellow diamonds* and *color-coded circles*, respectively. The *error bars* correspond to ±1 standard deviation (SD; note, for the average STCs in **C** and **D**, *error bars* are shown for every third point to improve readability of the figure). In **A**, an example of determination of low-side and high-side f_{cor} are shown with *closed* and *open triangles* (shifted vertically to avoid overlap), respectively. The probe frequency ranged from 0.93 to 1.44 kHz with an average of 1.09 kHz.

Specifically, the model consisted of two fixed factors (STC type with two levels: CAP vs SFOAE; experimental manipulation with four levels: baseline, three IT, or three acoustic overexposure frequencies) including interaction between them, one random factor (animal ID) and one covariate (the probe level). The probe level was included in the model as a covariate because it has been shown that SF-STC and CAP-STCs may exhibit broader tuning at higher probe levels (i.e., lower/higher low-/high-side corner frequencies; e.g., Dallos and Cheatham 1976a; Charaziak and Siegel 2014). A linear regression model accounting for within-subject variability was adapted to test whether the IT and acoustic trauma induced similar changes in the shapes of SF-STCs (Bland and Altman 1995). The data analysis was carried out in MATLAB (ver. R2010b, MathWorks) or in SPSS (ver. 22, IBM).

RESULTS

Baseline STCs—General Observations

The baseline 1-kHz CAP-STCs (n=21) were tuned similarly to CAP-STCs reported previously for chinchillas (Charaziak and Siegel 2014). The average quality factor Q_{10} (ratio of f_{probe} to the curve's bandwidth 10 dB above the tip) of CAP-STCs was

2.82 (SD=1.52), which is also similar to the Q_{10} of tuning curves of single-tone auditory nerve fibers in chinchillas at 1 kHz (Ruggero and Temchin 2005). The baseline CAP-STCs demonstrated other typical characteristics, including a minimum tuned to $f_{sup} \approx f_{probe}$ and a suppression threshold level at the tip below the probe level (Fig. 1B, D, black; e.g., Dallos and Cheatham 1976a).

Unlike CAP-STCs, the baseline SF-STCs were very broadly tuned, if at all. The Q_{10} values of baseline SF-STCs (average Q_{10}=0.44 with SD=0.35) were similar to those we obtained previously when calculated with the same methods (Charaziak and Siegel 2014). Other properties typical of 1-kHz SF-STCs in chinchillas were also observed, including tuning to $f_{sup} > f_{probe}$ (Fig. 1A, C, black) and rapid SFOAE residual phase accumulation at STC thresholds for $f_{sup} > f_{probe}$ (Fig. 2, black).

An interesting feature of baseline SF-STCs was a consistent increase in thresholds around f_{sup} 1–1.5 oct above f_{probe} (Fig. 1A, C, black). In the individual SF-STCs, this local increase in thresholds was usually aligned with a notch in SFOAE magnitude vs frequency functions (e.g., the notch near 2–3 kHz in Fig. 4C, black; for more discussion, see Charaziak and Siegel 2014).

Effects of the High-Frequency Interference Tones

We obtained 84 SF-STCs and 84 CAP-STCs from 21 animals, each animal contributing STCs for the four conditions (baseline, and with ITs of 9.2, 6.2, and 4.2 kHz). An example of a complete set of STC data for one animal is shown in Fig. 1A, B. For SF-STCs, there was little change in tuning properties between baseline (Fig. 1A, black) and the 9.2-kHz IT (red) condition. Addition of an IT at lower frequencies (6.2 and 4.2 kHz, blue and green, respectively) resulted in a progressive increase in the SF-STC thresholds on the high-frequency side with little or no change on the low-frequency side. In contrast, the CAP-STCs remained relatively unaffected by either IT (compare black vs colored curves in Fig. 1B). These trends were very consistent across all of the animals (see Fig. 1C, D for averaged STCs). The statistical significance of these observations was confirmed by an ANCOVA test. We found significant main effects and interaction between STC type and IT frequency on the high-side f_{cor} (Fig. 3A, $p<0.001$), but not on the low-side f_{cor} (Fig. 3B). Thus, while SF-STCs became progressively narrower with decreasing IT frequency due to changes in high-side f_{cor} but not low-side f_{cor}, no changes were observed for either f_{cor} of CAP-STCs. However, even with the lowest IT, the SF-STCs were broader than CAP-STCs as indicated by significant differences in high-side f_{cor} (by ~0.8 oct, Fig. 3A).

Effects of ITs on the high-frequency sides of SF-STCs were also observed in SFOAE residual phases at suppression threshold (Fig. 2A : individual data, : B average). There was little difference between SFOAE residual phase accumulation for the baseline and the 9.2-kHz IT condition (Fig. 2A, B, black and red curves, respectively), consistent with the lack of change in

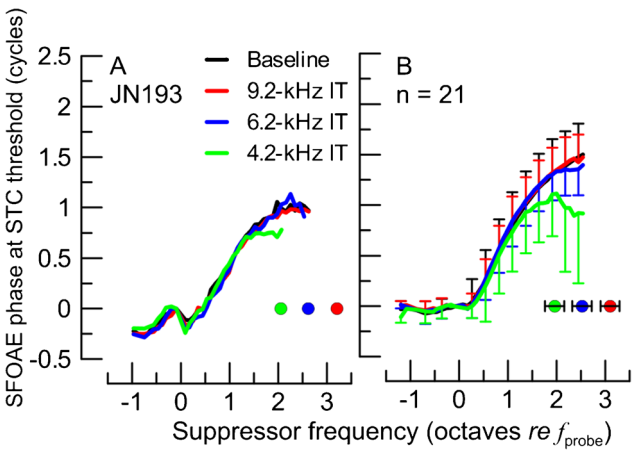

FIG. 2. The SFOAE residual phase at STC criterion threshold for baseline SF-STC (*black*) and for SF-STCs in presence of ITs at varying frequencies (see legend) in one animal (**A**) and averaged across 21 animals (**B**). Prior to averaging, the SFOAE residual phase curves were unwrapped and normalized to the phase value at the f_{sup} just below the f_{probe} to avoid effects of intersubject differences in the absolute phase. The frequencies of ITs are shown with *color-coded circles*. The *error bars* correspond to ±1 SD (note, for the average phase curve in **B**, *error bars* are shown for every third point, and for *black* and *red curves, error bars* are shown in the positive direction while for the other *two curves*, only for the negative direction).

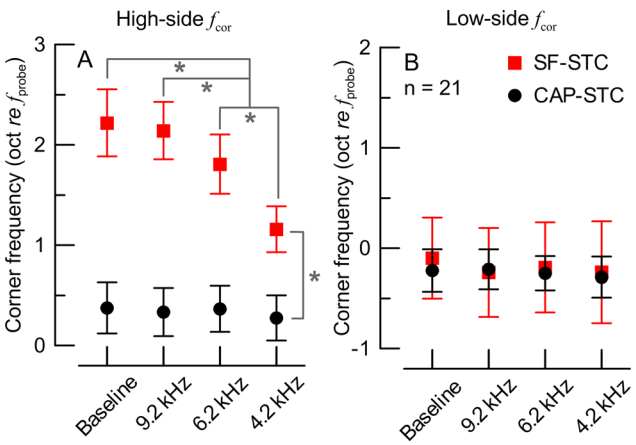

FIG. 3. Mean (±1 SD) corner frequencies (see *triangles* in Fig. 1A) for high-side (**A**) and low-side (**B**) of the tuning curves for CAP-STCs (*black*) and SF-STCs (*red*) recorded in the absence (*baseline*) and presence of the ITs (see *X*-axis). Data for 21 chinchillas. In **A**, the *brackets* and *asterisks* mark significant differences in the estimates of means and 95 % confidence intervals in the ANCOVA model (evaluated at a probe level of 39.1 dB SPL; the slope estimate for the probe level was 0.011 oct *re* f_{probe} per dB with standard error of 0.003). There were no significant differences in low-side f_{cor} (**B**).

thresholds of SF-STCs. However, although changes in the shapes of SF-STCs were observable for the 6.2-kHz IT condition (Fig. 1A, C, blue), there was little change in SFOAE residual phase at suppression threshold (Fig. 2, blue) as compared to the baseline data. When f_{sup} approached the IT frequency (4.2 kHz), the phase started to flatten for frequencies above the IT (Fig. 2, green) but remained unchanged below it. These results are consistent with the view that the IT suppressed SFOAE sources located basal but not apical to its CF place.

Effects of the Tonal Overexposures

Changes in CAP Thresholds and OAE Magnitudes. Of the 21 animals from which IT data were obtained, the acoustic trauma stage of the experiment was successfully completed for seven chinchillas.

The average CAP thresholds prior to and following tonal overexposures are shown in Fig. 4A. As intended, the subsequent exposures resulted in CAP threshold elevations of at least 70 dB SPL at the targeted frequencies (arrows) and above with little change in CAP thresholds below these frequencies. The CAP threshold shifts at the targeted frequencies averaged roughly 50 dB (Fig. 4B). Only the seven animals with CAP threshold shifts of at least 30 dB and/or CAP thresholds of at least 70 dB SPL at the targeted frequencies following each of the tonal exposures were included in the analyses. For these animals, the above requirement for CAP threshold shift/absolute threshold at targeted frequencies was maintained over the 2–2.5-h-long recording blocks between the exposures.

Following each of the exposures, the level versus frequency functions of SFOAEs were obtained with a probe level of 30 dB SPL across a wide frequency range (see Methods section). The tonal overexposures reduced SFOAE levels to the level of the noise in the targeted frequency regions (Fig. 4C). However, in two cases SFOAEs ~8–9 kHz started to recover during the subsequent lower frequency exposures, despite maintained CAP threshold shifts of more than 40 dB. This produced a small elevation in the average SFOAE level at ~8–9 kHz that persisted after the 5- and 3-kHz exposures (Fig. 4C, blue and green, respectively).

Changes in STCs. The analyses included 28 SF-STCs and 28 CAP-STCs. An example of an individual data set is shown in Fig. 5A (SF-STCs) and B (CAP-STCs). The effects of high-frequency acoustic trauma on the features of STCs were similar to the effects of the corresponding ITs (see Fig. 1): the CAP-STCs remained relatively unaffected by any of the expo-

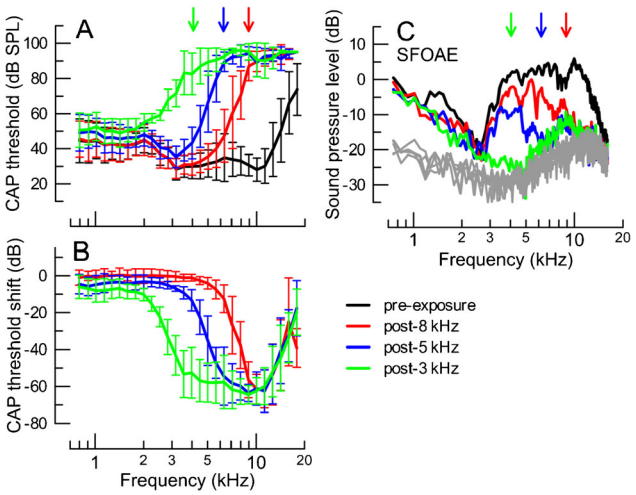

FIG. 4. Mean CAP thresholds prior to (*black*) and after exposing the animals to high-intensity tones in sequence, starting with a 8-kHz tone (*red*), then 5-kHz (*blue*) and lastly 3-kHz (*green*) for seven animals (**A**). The corresponding CAP threshold shifts (pre-exposure-post-exposure) are plotted in **B**. The *error bars* correspond to ±1 SD. In **C**, the average SFOAE levels evoked with a 30 dB SPL probe are shown across the frequency range, pre- and post-exposures. The noise levels are shown in *gray*. For clarity, the error bars were omitted in **C** (on average, the SD was 8 dB for SFOAE levels and 6 dB for the noise). The *arrows* in **A** and **C** indicate the targeted frequencies at which a CAP threshold of at least 70 dB SPL was expected following a given exposure (matching colors).

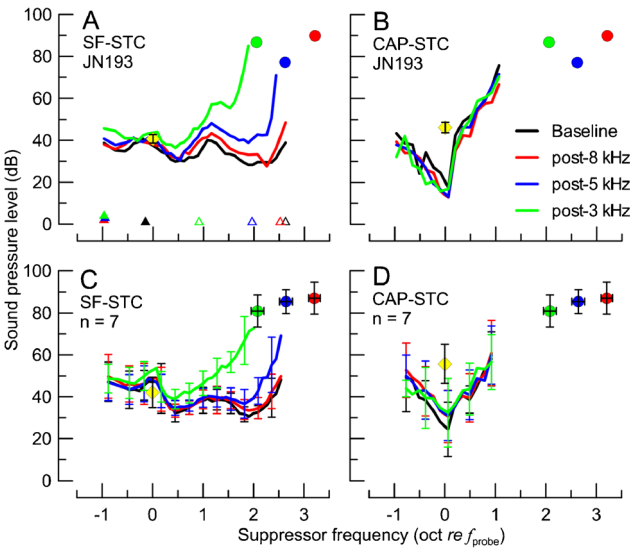

FIG. 5. The SF-STCs and CAP-STCs obtained for the baseline condition (*black*) and following the exposures to 8-kHz (*red*), 5-kHz (*blue*), and 3-kHz (*green*) tones for the animal previously shown in Fig. 1 (**A**, **B**) and averaged across seven animals (**C**, **D**). The parameters of the probe are shown with *yellow diamonds* (note, for clarity, a grand average of probe levels used across all conditions is shown; individual probe levels are listed in Table 2). The probe frequency ranged from 0.93 to 1.18 kHz with an average of 1.00 kHz. The *colored circles* show individual (**A**, **B**) or average (**C**, **D**) CAP thresholds at frequencies corresponding to ITs for a given animal. The error bars correspond to ±1 SD (note, for the average STCs in **C**, **D**, *error bars* are shown for every third point to improve readability). Corner frequencies are marked with triangles in **A** as in Fig. 1A.

sures but the high-frequency thresholds of SF-STCs became progressively higher as the acoustic trauma extended toward more apical locations. This behavior was also observed in the other six animals (averaged STCs in Fig. 5C, D). The SFOAE residual phase at the suppression criterion was affected by the exposures (data not shown) similarly as observed for the IT experiment (Fig. 2). The ANCOVA test revealed significant main effects and interaction of the STC type and tonal overexposure condition on the high-side f_{cor} ($p<0.001$; Fig. 6A) but not on the low-side f_{cor} (Fig. 6B). In summary, inducing acoustic trauma at frequencies ≥6 and ≥4 kHz led to progressively narrower SF-STC tuning due to increases in the slopes on the high-frequency side, while no significant changes in CAP-STC tuning were observed.

Comparison of the Effects of Tonal Overexposures and High-Frequency ITs

Within an individual, the IT SF-STCs had shapes similar to the corresponding post-exposure SF-STCs as shown in Fig. 7A for a typical animal (solid vs dotted lines in comparable colors). The degree of similarity between IT conditions and the corresponding post-exposure SF-STCs can be appreciated by calculating the difference between the suppressor levels at suppression threshold at each f_{sup}. As shown in Fig. 7B for a single animal and in Fig. 7C for averaged data, the differences between the SF-STCs measured with the IT and with acoustic exposures varied around 0 dB across the range of f_{sup}. In contrast, when the same subtraction procedure was applied to pairs of post-exposure SF-STCs (see black and gray brackets in the legend of Fig. 7), there were consistent deviations from 0 dB for the higher suppressor frequencies (Fig. 7B, C, black and gray). This indicates that the differences between pairs of IT and post-exposure SF-STCs were small compared to the changes that resulted from a given manipulation.

A linear regression model (described in Data Analyses section) applied to the high-side f_{cor} of post-exposure SF-STCs and the high-side f_{cor} of corresponding IT SF-STCs indicated that both types of manipulations affected SF-STCs similarly (Fig. 8).

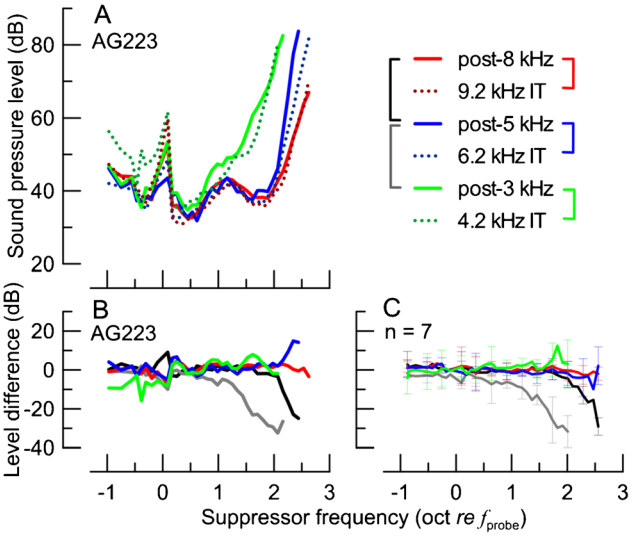

FIG. 7. The SF-STCs obtained for animal AG223 with the ITs present (**A**, *dotted*) and following exposures to intense tones (*solid*; see the legend). Note the similarity between the *solid* and *dotted curves*, plotted in similar colors, despite different manipulations (IT vs. exposure) and differences in probe levels used to measure SF-STCs (see Table 2). The differences (in dB) between the suppressor level at criterion threshold between pairs of SF-STCs for animal AG223 are shown in **B** (pairs of SF-STCs coded in colors as shown with brackets in the legend of **A**). Note the lack of consistent differences between post-exposure SF-STCs paired with IT SF-STCs (*colors*) as compared to the large differences on the high-frequency side between pairs of post-exposure SF-STCs (*black and gray*). The average SF-STC level differences for seven animals are shown in **C** (color code as in **B**). The *error bars* show ±1 SD; note, to preserve the clarity, *error bars* are shown only for every third data point.

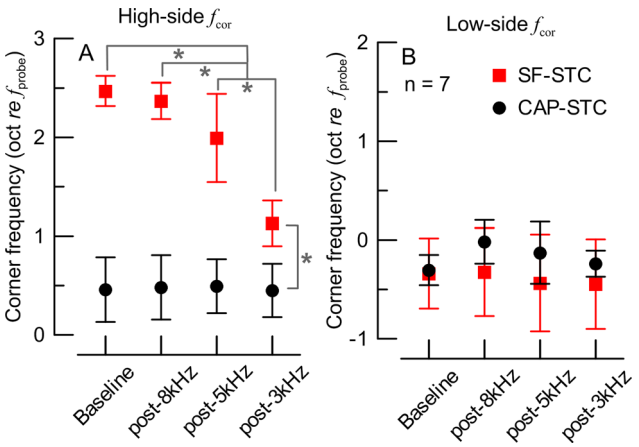

FIG. 6. Mean (±1 SD) corner frequencies for the high-side (**A**) and low-side (**B**) of the tuning curves for CAP-STCs (*black*) and SF-STCs (*red*) measured before (*baseline*) and following tonal-exposures (*X*-axis). Data for seven chinchillas. In **A**, the *brackets* and *asterisks* mark significant differences in the estimates of means and 95 % confidence intervals in the ANCOVA model (evaluated at a probe level of 48.9 dB SPL; the slope estimate for the probe level was 0.016 oct *re* f_{probe} per dB with SE=0.005). There were no significant differences in low-side f_{cor} (**B**).

DISCUSSION

Broad Region of SFOAE Generation at Low Frequencies

The tuning of 1-kHz SF-STCs changed from a broad to narrow band-pass shape upon addition of ITs and following acoustic trauma. In contrast, neither of these manipulations affected the tuning of CAP-STCs establishing that they did not exert their effects near

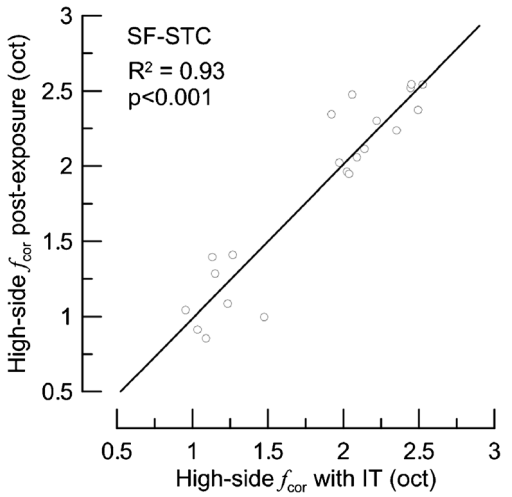

FIG. 8. The high-side corner frequencies (oct *re* f_{probe}) of SF-STCs collected in the presence of ITs (*X*-axis) compared with corresponding corner frequencies of SF-STCs collected in the same animal following acoustic trauma (*Y*-axis). Data for seven animals. The *solid line* represents the fit of the linear regression model (the slope estimate was equal to 1.024, SE=0.083, and the intercept estimate was not significantly different from zero).

the 1-kHz CF place of the probe. These results suggest that there are sizable contributions to SFOAEs evoked by 1-kHz tones from sources extending somewhere between 6.4 to 7.7 mm (2.5 to 3 oct) basal to the 1-kHz place as we observed significant changes in SF-STCs due to manipulations to the region of the 6-kHz place but not to the region of the 9-kHz place (Figs. 3A and 6A; based on cochlear map from Muller et al. 2010). Thus, generation of 1-kHz SFOAEs seems to involve 30 to 40 % of the cochlear length in chinchillas. Some SFOAE sources generating emissions below our SF-STC threshold criterion (0 dB SPL) could be still present even beyond that region though. Although these estimates are specific to the 1-kHz probe tones used in this study, it is reasonable to assume that the concept of SFOAEs originating over an extended region applies to other frequencies at which SF-STCs were broadly tuned (<3 kHz in chinchillas; Charaziak and Siegel 2014).

If the broad region of SFOAE generation is exaggerated at low frequencies in other species as well, then broad, essentially high-pass tuning of SF-STCs should be observable at these frequencies. Although data are sparse, there are a few reports supporting this view, if one considers that the term "low frequency" may apply to different frequency ranges in different species (see next section). For instance, Cheatham et al. (2011b) reported that while SF-STCs of wild-type mice can be as sharp as auditory nerve fiber threshold tuning curves, "the use of moderate-level, low-frequency probes can make it difficult to obtain the steep high-frequency slope of the (SFOAE) tuning functions," plausibly reflecting contributions from basally located OAE sources. Human SF-STCs have narrow band-pass shapes for probe frequencies of 0.75–1 kHz and above (Kemp and Chum 1980; Brass and Kemp 1993; Keefe et al. 2008; Charaziak et al. 2013), while at 0.5 kHz, Keefe et al. (2008) reported SF-STCs without well-defined high-frequency sides. These data must be interpreted with caution as the shapes of 0.5 kHz SF-STCs were not followed for suppressor frequencies beyond 0.7 oct above the probe frequency. The most direct indication that low-frequency SFOAEs in humans may have a broad region of generation has been provided by iso-input suppression data (Baiduc et al. 2012). Whereas at high probe frequencies, the suppressors near the probe are far more effective (i.e., revealing larger SFOAE residuals), at lower frequencies (<0.7 kHz) suppressors even an octave above the probe can be as effective as those near the probe. An extended region of SFOAE generation may also explain significant off-frequency correlations between SFOAEs (0.5–2 kHz) and higher frequency audiometric thresholds (Avan et al. 1991; Ellison and Keefe 2005). Although SF-STCs have not been measured in other mammals, suppression of low-frequency SFOAEs (<3–4 kHz) in cats and guinea pigs by tones over an octave higher are consistent with a broad generation region in these species as well (Guinan 1990; Souter 1995).

Differences in Low- Versus High-Frequency Cochlear Responses Are Not Specific to SF-STCs

The frequency marking a transition from broad to narrow band-pass SF-STCs tuning (~3 kHz) seem to correspond to a break in the trend of SFOAE group delay versus frequency, where at lower frequencies, the group delays were shorter than the predicted OAE round-trip travel times derived from basilar membrane data in chinchillas (Siegel et al. 2005). Shorter than expected SFOAE group delays were also measured in cats and guinea pigs for frequencies below 3 kHz (Shera and Guinan 2003; Siegel et al. 2005; Shera et al. 2010). Although basilar membrane data are not available for humans and mice, there also seems to be break in SFOAE group delays around 1–2 and 10–15 kHz, respectively (Siegel 2008; Shera et al. 2010). In agreement with the human SFOAE data, Rasetshwane et al. (2013) reported that latencies of TEOAEs were shorter than forward travel times extracted from auditory brainstem responses at frequencies below 1.5 kHz, while the opposite trend was observed at higher frequencies. It has been proposed that this break in SFOAE group delays marks a transition between basal- and apical-like behaviors (Shera and Guinan 2003; Shera et al. 2010). Importantly, because the frequency of the apical-basal transition seems to vary across species, interspecies

comparisons of the properties of SFOAEs at the same absolute frequency may exaggerate the differences (e.g., comparing 1-kHz SF-STCs in humans and chinchillas would correspond to comparing basal-like to apical-like SF-STCs, respectively). Although DPOAEs are thought to be generated in part via different mechanisms than SFOAEs and TEOAEs (e.g., Shera and Guinan 1999), their phase profiles also suggest a transition between so called "scaling" and "nonscaling" cochlear behavior for stimuli around 4 kHz for chinchillas and around 1–2 kHz in humans (e.g., Dhar et al. 2011; Martin et al. 2011). Yet, DP-STCs measured across a wide frequency range in humans do not appear to reflect this transition as they are tuned similarly even for the lowest frequencies tested, i.e., ~0.5 kHz (Gorga et al. 2011; see next section for more discussion).

The apical-basal transition is not specific to OAEs and can be observed in other types of cochlear responses. Temchin et al. (2008) showed that while frequency-threshold tuning curves from auditory nerve fibers in chinchillas remain V-shaped throughout the whole tested frequency range (unlike SF-STCs), they also undergo a change in shape for CFs around 3–4 kHz, where distinct tip and tail regions are evident at higher frequencies. Similar changes in the tuning curves of single units can be observed around 3 kHz in cats and guinea pigs and around 15 kHz in mice (Evans 1972; Liberman 1978; Taberner and Liberman 2005). Based on changes in spatial trajectories of inner hair cell depolarization derived from auditory nerve responses in chinchillas, Temchin et al. (2012) hypothesized that a second forward traveling wave is launched in the apical-basal transition region simultaneously with the "classical" traveling wave for low-frequency sounds. This second traveling wave may be related to short SFOAE group delays and broad SFOAE tuning at low frequencies, but a plausible mechanism has yet to be discovered. Some models explain the generation of short-latency OAEs via a reflection mechanism located basal to the CF place of the stimulus (Choi et al. 2008; Moleti et al. 2013). However, these models do not account for apparent differences between apical and basal cochlear responses, and thus do not specifically explain an "exaggerated" SFOAE generation region for low-frequency probes.

Broad Region of Generation of OAEs Evoked with Complex Stimuli

The idea of emissions being generated over a broad region of the cochlea is neither new nor unique to SFOAEs. For instance, tones or tone bursts remote from the frequency of the evoking sound can suppress TEOAEs, suggesting that the generators are distributed over a broader region of the cochlea (Sutton 1985; Zwicker and Wesel 1990; Zettner and Folsom 2003; Killan et al. 2012; Lewis and Goodman 2014). Differences in growth functions of short- and long-latency components of TEOAEs support the idea that the former component originated in more basal locations (Goodman et al. 2011; Sisto et al. 2013). This interpretation is also indicated by time-frequency analysis of TEOAEs obtained in ears with steep audiometric threshold cutoffs at high frequencies (Moleti et al. 2014). In line with this hypothesis, damage to the basal locations of the cochlea has been shown to affect TEOAEs at low- and mid-frequencies and significant correlations have been reported between high-frequency audiometric thresholds and the amplitudes of TEOAE spectra at lower frequencies (Avan et al. 1993, 1995, 1997; Withnell et al. 2000; Murnane and Kelly 2003; Jedrzejczak et al. 2012; Moleti et al. 2014). Although Mertes and Goodman (2013) did not find strong correlations between a short-latency component of the TEOAE and higher frequency audiometric thresholds (possibly due to a limited range/sparse sampling of included test frequencies), their results support the idea of long- and short-latency components originating at different cochlear locations.

On the other hand, narrow band-pass tuning of human DP-STCs does not support the idea of contributions from basal sources, at least for DPOAEs (e.g., Gorga et al. 2011). However, it has been shown that basal contributions to DPOAEs may produce variable effects on STCs, where a secondary lobe of either suppression or enhancement can be observed for high-frequency f_{sup} for certain stimulus conditions rather than the very broad tuning evident in SF-STCs (Martin et al. 1999; Mills 2000; Martin et al. 2003). Thus, the methodological approach for constructing DP-STCs is crucial to inferring the region where DPOAEs are generated. Importantly, studies free of this limitation such as noise exposure experiments, correlations between DPOAEs, and hearing thresholds, as well as other DPOAE suppression characteristics, support the existence of basal DPOAE sources (e.g., Arnold et al. 1999; Harding et al. 2002; Dreisbach et al. 2008; Martin et al. 2009, 2010, 2011).

Thus, even though emissions evoked with different acoustic stimuli most likely include contributions from different generation mechanisms (Shera and Guinan 1999; Yates and Withnell 1999; Martin et al. 2011), to some degree, an extended region of generation seems to be common for all types of evoked OAEs. Whether the generation mechanisms behind the basal OAE sources are the same across species and the evoking stimulus conditions remain to be evaluated.

The Effects of Tonal Exposures on the Cochlea

The short-duration tonal exposures resulted in ~50 dB CAP threshold shifts (Fig. 4B), likely because

of a decrease in efficiency of OHC mechanotransduction and thus decreased mechanical feedback (Ruggero et al. 1996). In support of this view, we observed a drop in cochlear microphonic (CM) residuals following the exposures (data not shown) that generally followed the same trends as SFOAE levels shown in Fig. 4C (note, CM residuals were collected simultaneously and with the same procedures as SFOAEs). The decreased CM residual amplitudes presumably reflect a drop in the OHC receptor currents in the affected regions (e.g., Dallos and Cheatham 1976b; Cheatham et al. 2011a). While histological evaluation of exposed cochleae was not performed, it is presumed there was little permanent damage to the organ of Corti and the sensitivity loss was mostly temporary in nature as previously shown for similar short-duration tonal exposures (e.g., Liberman and Dodds 1987; Clark 1991; Ruggero et al. 1996; Nordmann et al. 2000). This is important, as the presence of extensive lesions in the organ of Corti has been associated with the creation of new "damage-evoked" OAEs corresponding to the edges of the damaged region (e.g., possibly due to impedance mismatch, Zurek and Clark 1981; Clark et al. 1984). There was also no increase in SFOAE levels near the frequency ranges where thresholds varied rapidly with stimulus frequency (Fig. 4A, C). Thus, it is unlikely that damage-evoked emissions were created and interacted with SF-STCs. In summary, we conclude that the changes in SF-STC tuning caused by high to mid-frequency acoustic trauma reflected reduced generation of SFOAEs in the affected regions, most likely related to reduced OHC transducer currents.

Interactions Between Suppressors and the Interference Tones

When measuring an SF-STC in the presence of a high-frequency IT, one must take into consideration the possibility of interactions between the fixed IT and the varying suppressor. Although it was assured that distortion products created between IT and f_{sup} did not coincide with the f_{probe}, another issue could have arisen when f_{sup} and IT were close in frequency, as the intracochlear responses to either tone could be diminished due to mutual suppression (e.g., Rhode 2007). Whereas the f_{sup} was unlikely to suppress the response to the IT (for f_{sup}<IT) due to the large level difference (i.e., thresholds for low-side suppression were relatively high), the opposite may have occurred. Based on Rhode's (2007) basilar membrane measurements in chinchillas, it would be expected to observe 5–10 dB decrease in the intracochlear response to an intense 3.8-kHz f_{sup} due to the presence of 4.2-kHz IT at 75 dB SPL, which is not enough to explain the observed elevation in the suppression threshold (compare black vs green SF-STC thresholds at f_{sup} of 1.9 oct in Fig. 1A).

The use of high-frequency tones to saturate SFOAE sources has been criticized based on a model that combined coherent linear reflection and nonlinear distortion mechanisms. The model predicts that the suppressor itself may create new probe frequency SFOAE sources by inducing mechanical perturbations and/or sources of nonlinear distortion (Shera et al. 2004). Although this possibility cannot be definitively ruled out, the similarity of effects of ITs and acoustic trauma on SF-STC tuning (Fig. 8) makes this alternate explanation unlikely.

Summary

The primary aim of this study was to follow up on results of (Charaziak and Siegel 2014) where it has been shown that SF-STCs were over five times broader than CAP-STCs at probe frequencies below 3 kHz in chinchillas. The hypothesis that broad tuning of low-frequency SF-STCs was due to a broad region of SFOAE generation extending basal to the CF of the low-level probe tone was tested. Manipulations to basal and middle regions of the cochlea by ITs or acoustic trauma resulted in increased high-frequency thresholds of the 1-kHz SF-STCs but did not affect the 1-kHz CAP-STCs. Similarity of the effects of the ITs and corresponding acoustic trauma on SF-STC tuning suggests that both manipulations affected OAE sources in an analogous way, although probably via different mechanisms (e.g., transducer saturation vs reduction of transducer current). Both mechanisms would reduce the transducer current at the probe frequency. If SFOAEs are generated in the transducer or via a cellular mechanism closely tied to transduction, then the most economical conclusion is that suppressors suppress but do not generate new contributions to SFOAEs. In summary, the results support the hypothesis that SFOAEs evoked by low-frequency tones are generated over a broad region of the cochlea corresponding to 30–40 % of its length. The lack of effects of the experimental manipulations on CAP-STCs strongly supports the interpretation that neither the IT nor the effects of acoustic trauma were manifested in the region of the characteristic place of the probe.

ACKNOWLEDGMENTS

This study was supported by the NIH Grant DC-00419 (M. Ruggero), Northwestern University School of Communication Ignition grant, and Northwestern University. We thank Dr. Sumitrajit Dhar and Dr. Steven Zecker for statistical consultations.

REFERENCES

ARNOLD DJ, LONSBURY-MARTIN BL, MARTIN GK (1999) High-frequency hearing influences lower-frequency distortion-product otoacoustic emissions. Arch Otolaryngol Head Neck Surg 125:215–222

AVAN P, BONFILS P, LOTH D, NARCY P, TROTOUX J (1991) Quantitative assessment of human cochlear function by evoked otoacoustic emissions. Hear Res 52:99–112

AVAN P, BONFILS P, LOTH D, WIT HP (1993) Temporal patterns of transient-evoked otoacoustic emissions in normal and impaired cochleae. Hear Res 70:109–120

AVAN P, BONFILS P, LOTH D, ELBEZ M, ERMINY M (1995) Transient-evoked otoacoustic emissions and high-frequency acoustic trauma in the guinea pig. J Acoust Soc Am 97:3012–3020

AVAN P, ELBEZ M, BONFILS P (1997) Click-evoked otoacoustic emissions and the influence of high-frequency hearing losses in humans. J Acoust Soc Am 101:2771–2777

BAIDUC R, CHARAZIAK KK, SIEGEL JH (2012) Spatial distribution of stimulus-frequency otoacoustic emissions generators in humans. Assoc Res Otolaryngol Abstr 398 35

BLAND JM, ALTMAN DG (1995) Calculating correlation coefficients with repeated observations: part 1—correlation within subjects. BMJ 310:446

BRASS D, KEMP DT (1993) Suppression of stimulus frequency otoacoustic emissions. J Acoust Soc Am 93:920–939

CHARAZIAK KK, SIEGEL JH (2014) Estimating cochlear frequency selectivity with stimulus-frequency otoacoustic emissions in chinchillas. J Assoc Res Otolaryngol 15:883–896

CHARAZIAK KK, SOUZA P, SIEGEL JH (2013) Stimulus-frequency otoacoustic emission suppression tuning in humans: comparison to behavioral tuning. J Assoc Res Otolaryngol 14:843–862

CHEATHAM MA, NAIK K, DALLOS P (2011A) Using the cochlear microphonic as a tool to evaluate cochlear function in mouse models of hearing. J Assoc Res Otolaryngol 12:113–125

CHEATHAM MA, KATZ ED, CHARAZIAK KK, DALLOS P, SIEGEL JH (2011B) Using stimulus frequency emissions to characterize cochlear function in mice. AIP Conf Proc 1403:383–388

CHOI YS, LEE SY, PARHAM K, NEELY ST, KIM DO (2008) Stimulus-frequency otoacoustic emission: measurements in humans and simulations with an active cochlear model. J Acoust Soc Am 123:2651–2669

CLARK WW (1991) Recent studies of temporary threshold shift (TTS) and permanent threshold shift (PTS) in animals. J Acoust Soc Am 90:155–163

CLARK WW, KIM DO, ZUREK PM, BOHNE BA (1984) Spontaneous otoacoustic emissions in chinchilla ear canals: correlation with histopathology and suppression by external tones. Hear Res 16:299–314

DALLOS P, CHEATHAM MA (1976A) Compound action potential (AP) tuning curves. J Acoust Soc Am 59:591–597

DALLOS P, CHEATHAM MA (1976B) Production of cochlear potentials by inner and outer hair cells. J Acoust Soc Am 60:510–512

DAVIS RI, AHROON WA, HAMERNIK RP (1989) The relation among hearing loss, sensory cell loss and tuning characteristics in the chinchilla. Hear Res 41:1–14

DHAR S, ROGERS A, ABDALA C (2011) Breaking away: violation of distortion emission phase-frequency invariance at low frequencies. J Acoust Soc Am 129:3115–3122

DREISBACH LE, TORRE P 3RD, KRAMER SJ, KOPKE R, JACKSON R, BALOUGH B (2008) Influence of ultrahigh-frequency hearing thresholds on distortion-product otoacoustic emission levels at conventional frequencies. J Am Acad Audiol 19:325–336

ELLISON JC, KEEFE DH (2005) Audiometric predictions using stimulus-frequency otoacoustic emissions and middle ear measurements. Ear Hear 26:487–503

EVANS EF (1972) The frequency response and other properties of single fibres in the guinea-pig cochlear nerve. J Physiol 226:263–287

GEISLER CD, YATES GK, PATUZZI RB, JOHNSTONE BM (1990) Saturation of outer hair cell receptor currents causes two-tone suppression. Hear Res 44:241–256

GOODMAN SS, MERTES IB, SCHEPERLE RA (2011) Delays and growth rates of multiple TEOAE components. In: Shera CA, Olson ES (eds) What fire is in mine ears: progress in auditory biomechanics. AIP Conf. Proc, pp 279–285

GORGA MP, NEELY ST, KOPUN J, TAN H (2011) Distortion-product otoacoustic emission suppression tuning curves in humans. J Acoust Soc Am 129:817–827

GUINAN JJ (1990) Changes in stimulus frequency otoacoustic emissions produced by two-tone suppression and efferent stimulation in cats. In: Dallos P, Geisler CD, Matthews JW, Ruggero MA, Steele CR (eds) The mechanics and biophysics of hearing. Springer, Madison, pp 170–177

HARDING GW, BOHNE BA, AHMAD M (2002) DPOAE level shifts and ABR threshold shifts compared to detailed analysis of histopathological damage from noise. Hear Res 174:158–171

HE W, PORSOV E, KEMP D, NUTTALL AL, REN T (2012) The group delay and suppression pattern of the cochlear microphonic potential recorded at the round window. PLoS One 7:e34356

HEITMANN J, WALDMANN B, SCHNITZLER H-U, PLINKERT PK, ZENNER H-P (1998) Suppression of distortion product otoacoustic emissions (DPOAE) near 2f1–f2 removes DP-gram fine structure—evidence for a secondary generator. J Acoust Soc Am 103:1527–1531

JEDRZEJCZAK WW, KOCHANEK K, TRZASKOWSKI B, PILKA E, SKARZYNSKI PH, SKARZYNSKI H (2012) Tone-burst and click-evoked otoacoustic emissions in subjects with hearing loss above 0.25, 0.5, and 1 kHz. Ear Hear 33:757–767

KALLURI R, SHERA CA (2007) Comparing stimulus-frequency otoacoustic emissions measured by compression, suppression, and spectral smoothing. J Acoust Soc Am 122:3562–3575

KEEFE DH, ELLISON JC, FITZPATRICK DF, GORGA MP (2008) Two-tone suppression of stimulus frequency otoacoustic emissions. J Acoust Soc Am 123:1479–1494

KEMP DT (2007) Otoacoustic Emissions: the basics, the science and the future potential. In: Robinette MS, Glattke TJ (eds) Otoacoustic emissions: clinical applications. Theime, New York, pp 7–42

KEMP DT, CHUM RA (1980) Observations on the generator mechanism of stimulus frequency acoustic emissions–two tone suppression. In: deBoer E, Viergever MA (eds) Psychophysical, physiological and behavioral studies in hearing. Delft University Press, Delft, pp 34–41

KILLAN EC, LUTMAN ME, MONTELPARE WJ, THYER NJ (2012) A mechanism for simultaneous suppression of tone burst-evoked otoacoustic emissions. Hear Res 285:58–64

LEWIS J, GOODMAN S (2014) The origin of short-latency transient-evoked otoacoustic emissions. J Assoc Res Otolaryngol 37:72, Abstr: 126

LIBERMAN MC (1978) Auditory-nerve response from cats raised in a low-noise chamber. J Acoust Soc Am 63:442–455

LIBERMAN MC, DODDS LW (1987) Acute ultrastructural changes in acoustic trauma: serial-section reconstruction of stereocilia and cuticular plates. Hear Res 26:45–64

MARTIN GK, STAGNER BB, JASSIR D, TELISCHI FF, LONSBURY-MARTIN BL (1999) Suppression and enhancement of distortion-product otoacoustic emissions by interference tones above f(2). I. Basic findings in rabbits. Hear Res 136:105–123

MARTIN GK, VILLASUSO EI, STAGNER BB, LONSBURY-MARTIN BL (2003) Suppression and enhancement of distortion-product otoacoustic emissions by interference tones above f(2). II. Findings in humans. Hear Res 177:111–122

Martin GK, Stagner BB, Fahey PF, Lonsbury-Martin BL (2009) Steep and shallow phase gradient distortion product otoacoustic emissions arising basal to the primary tones. J Acoust Soc Am 125:El85–El92

Martin GK, Stagner BB, Lonsbury-Martin BL (2010) Evidence for basal distortion-product otoacoustic emission components. J Acoust Soc Am 127:2955–2972

Martin GK, Stagner BB, Chung YS, Lonsbury-Martin BL (2011) Characterizing distortion-product otoacoustic emission components across four species. J Acoust Soc Am 129:3090–3103

Mertes IB, Goodman SS (2013) Short-latency transient-evoked otoacoustic emissions as predictors of hearing status and thresholdsa). J Acoust Soc Am 134:2127–2135

Mills DM (2000) Frequency responses of two- and three-tone distortion product otoacoustic emissions in Mongolian gerbils. J Acoust Soc Am 107:2586–2602

Moleti A, Al-Maamury AM, Bertaccini D, Botti T, Sisto R (2013) Generation place of the long- and short-latency components of transient-evoked otoacoustic emissions in a nonlinear cochlear model. J Acoust Soc Am 133:4098–4108

Moleti A, Sisto R, Lucertini M (2014) Experimental evidence for the basal generation place of the short-latency transient-evoked otoacoustic emissions. J Acoust Soc Am 135:2862–2872

Muller M, Hoidis S, Smolders JW (2010) A physiological frequency-position map of the chinchilla cochlea. Hear Res 268:184–193

Murnane OD, Kelly JK (2003) The effects of high-frequency hearing loss on low-frequency components of the click-evoked otoacoustic emission. J Am Acad Audiol 14:525–533

Neely S, Liu Z (2011) EMAV: otoacoustic emission averager. In: Technical Memorandum. Omaha, NE: Boys Town National Research Hospital

Nordmann AS, Bohne BA, Harding GW (2000) Histopathological differences between temporary and permanent threshold shift. Hear Res 139:13–30

Özdamar Ö, Dallos P (1978) Synchronous responses of the primary auditory fibers to the onset of tone burst and their relation to compound action potentials. Brain Res 155:169–175

Pickles JO, Osborne MP, Comis SD (1987) Vulnerability of tip links between stereocilia to acoustic trauma in the guinea pig. Hear Res 25:173–183

Puel JL, Bobbin RP, Fallon M (1988) The active process is affected first by intense sound exposure. Hear Res 37:53–63

Rasetshwane DM, Argenyi M, Neely ST, Kopun JG, Gorga MP (2013) Latency of tone-burst-evoked auditory brain stem responses and otoacoustic emissions: level, frequency, and rise-time effects. J Acoust Soc Am 133:2803–2817

Rhode WS (2007) Mutual suppression in the 6 kHz region of sensitive chinchilla cochleae. J Acoust Soc Am 121:2805–2818

Ruggero MA, Temchin AN (2005) Unexceptional sharpness of frequency tuning in the human cochlea. Proc Natl Acad Sci U S A 102:18614–18619

Ruggero MA, Rich NC, Recio A (1996) The effect of intense acoustic stimulation on basilar-membrane vibrations. Audit Neurosci 2:329–345

Shera CA, Guinan JJ Jr (1999) Evoked otoacoustic emissions arise by two fundamentally different mechanisms: a taxonomy for mammalian OAEs. J Acoust Soc Am 105:782–798

Shera CA, Guinan JJ Jr (2003) Stimulus-frequency-emission group delay: a test of coherent reflection filtering and a window on cochlear tuning. J Acoust Soc Am 113:2762–2772

Shera CA, Tubis A, Talmadge CL, Guinan JJ Jr (2004) The dual effect of "suppressor" tones on stimulus-frequency otoacoustic emissions. J Assoc Res Otolaryngol 27:538

Shera CA, Guinan JJ Jr, Oxenham AJ (2010) Otoacoustic estimation of cochlear tuning: validation in the chinchilla. J Assoc Res Otolaryngol 11:343–365

Siegel JH (2006) The biophysical origin of otoacoustic emissions. In: Nuttall AL, Ren T, Gillespe P, Grosh K, de Boer E (eds) Auditory mechanisms: processes and models. World Scientific, Singapore, pp 361–368

Siegel JH (2007) Calibration of otoacoustic emission probes. In: Robinette MS, Glattke TJ (eds) Otoacoustic emissions: clinical applications, 3rd edn. Thieme, New York, pp 403–429

Siegel JH (2008) Species differences in low-level otoacoustic emissions may be explained by "hot regions" in the cochlea. J Acoust Soc Am 123:3852

Siegel JH, Cerka AJ, Recio-Spinoso A, Temchin AN, van Dijk P, Ruggero MA (2005) Delays of stimulus-frequency otoacoustic emissions and cochlear vibrations contradict the theory of coherent reflection filtering. J Acoust Soc Am 118:2434–2443

Sisto R, Sanjust F, Moleti A (2013) Input/output functions of different-latency components of transient-evoked and stimulus-frequency otoacoustic emissions. J Acoust Soc Am 133:2240–2253

Songer JE, Rosowski JJ (2005) The effect of superior canal dehiscence on cochlear potential in response to air-conducted stimuli in chinchilla. Hear Res 210:53–62

Souter M (1995) Stimulus frequency otoacoustic emissions from guinea pig and human subjects. Hear Res 90:1–11

Sutton GJ (1985) Suppression effects in the spectrum of evoked oto-acoustic emissions. Acustica 58:57–63

Taberner AM, Liberman MC (2005) Response properties of single auditory nerve fibers in the mouse. J Neurophysiol 93:557–569

Teas DC, Eldredge DH, Davis H (1962) Cochlear responses to acoustic transients: an interpretation of whole-nerve action potentials. J Acoust Soc Am 34:1438–1459

Temchin AN, Rich NC, Ruggero MA (2008) Threshold tuning curves of chinchilla auditory-nerve fibers. I. Dependence on characteristic frequency and relation to the magnitudes of cochlear vibrations. J Neurophysiol 100:2889–2898

Temchin AN, Recio-Spinoso A, Cai H, Ruggero MA (2012) Traveling waves on the organ of Corti of the chinchilla cochlea: spatial trajectories of inner hair cell depolarization inferred from responses of auditory-nerve fibers. J Neurosci 32:10522–10529

Thorne PR, Duncan CE, Gavin JB (1986) The pathogenesis of stereocilia abnormalities in acoustic trauma. Hear Res 21:41–49

Withnell RH, Yates GK, Kirk DL (2000) Changes to low-frequency components of the TEOAE following acoustic trauma to the base of the cochlea. Hear Res 139:1–12

Yates GK, Withnell RH (1999) The role of intermodulation distortion in transient-evoked otoacoustic emissions. Hear Res 136:49–64

Zettner EM, Folsom RC (2003) Transient emission suppression tuning curve attributes in relation to psychoacoustic threshold. J Acoust Soc Am 113:2031–2041

Zurek PM, Clark WW (1981) Narrow-band acoustic-signals emitted by chinchilla ears after noise exposure. J Acoust Soc Am 70:446–450

Zweig G, Shera CA (1995) The origin of periodicity in the spectrum of evoked otoacoustic emissions. J Acoust Soc Am 98:2018–2047

Zwicker E, Wesel J (1990) The effect of addition in suppression of delayed evoked otoacoustic emissions and in masking. Acta Acustica 70:189–196